HYDRAULIC MODEL STUDY OF OIL/GRIT SEPARATOR

Final Report

by

Terry W. Sturm, Jed Costanza, and Kurt Pennell
School of Civil and Environmental Engineering
Georgia Institute of Technology
Atlanta, GA 30332

Submitted to

SKIMPRO Technologies
Duluth, Georgia

March 2007

ACKNOWLEDGMENTS

Construction and operation of the model was carried out with the expert assistance of Andy Udell, Hydraulics Lab Coordinator. Velocity measurements were conducted by graduate students Joshua Robinson and SeungOh Lee. Undergraduate students Allen Peninger and Marcin Kolesinski provided assistance with analysis of the sediment samples.

EXECUTIVE SUMMARY

Experimental tests of a 1:2 scale model of an oil/grit separator designed by Skimpro Technologies of Duluth, Georgia were conducted in the Hydraulics Laboratory at the Georgia Institute of Technology. A recirculation system with a large sedimentation tank downstream of the separator was set up so that oil and grit could be continuously fed to the separator through the inlet pipe and trap efficiencies could be measured. In addition, detailed velocity distributions were measured inside the oil/grit separator to visualize the flow patterns for different baffle arrangements and to explain differences in oil and grit removal efficiency.

The specific objective of Phase 1 of this study was to measure the removal efficiency of grit and oil in the model to evaluate the existing design and suggest possible design improvements. In Phase 2 of the study, various modifications of the internal baffles of the separator were tested to optimize both oil and grit removal for one grit size and one representative flow rate. For the chosen final design modification, the same grit sizes and range of input flow rates utilized in Phase 1 of the study were repeated in a full series of tests to provide a comparison of the performance of the modified structure to that of the existing design as tested in Phase 1. Design performance was evaluated as the percent of incoming oil or grit trapped in the separator as a function of the surface loading rate (flow rate in cfs per ft^2 of surface area) applied to the separator.

In the Phase 1 tests, the oil trap efficiency exceeded 80 percent at a surface loading rate of 0.032 cfs/ft^2, but it declined very rapidly for surface loading rates greater than 0.032 cfs/ft^2. This significant deficiency in performance of the oil/grit separator was remedied by Modification IV (Mod IV) in the Phase 2 tests through alteration of the internal velocity distributions by modifying the grit baffle flow openings. The oil trap efficiencies for Mod IV were higher than those for Phase 1 tests over an extended range of surface loading rates up to values of nearly 0.06 cfs/ft^2. At a surface loading rate of 0.042 cfs/ft^2, for example, the oil trap efficiency increased from approximately 45 percent in Phase 1 to 72 percent for Mod IV in Phase 2 which was an increase by a factor of 1.6. In terms of maintaining a minimum oil trap efficiency of 40 percent, the Mod IV design extended maximum allowable flow rates by 25 percent in comparison to the Phase 1 results. The Mod IV design also significantly reduced oil concentrations near the water surface at the outlet of the Skimpro separator.

Trap efficiencies for three different sands with median sizes of 0.12 mm, 0.17 mm, and 0.30 mm were greater than 80 percent at a surface loading rate of 0.016 cfs/ft^2 for both Phase 1 and Mod IV results. At a suggested maximum design loading rate of 0.036 cfs/ft^2, the grit trap efficiency exceeded 40 percent for all three sand sizes tested in the Phase 1 and the Mod IV configurations. This performance meets or exceeds current suggested design guidelines for total suspended solids (TSS) removal by oil/grit separators.

These test results demonstrated successful improvement of the Skimpro oil/grit separator because performance of the Mod IV design was shown to be more robust for both oil and grit removal over a wider range of flow rates. Optimization of the oil/grit separator for both oil and grit removal in this study has resulted in a structural BMP that can effectively reduce both TSS and hydrocarbon releases in urban runoff from industrial and commercial impervious surfaces into surface water bodies.

TABLE OF CONTENTS

LIST OF FIGURES

LIST OF TABLES

CHAPTER 1.

INTRODUCTION

Stormwater runoff from parking lots and paved roadway surfaces contains grit and oil that can cause water quality problems downstream of the discharge point. Under these circumstances, it is desirable to utilize a structural best management practice (BMP) for improvement of the water quality of the effluent. The difficulty in using such BMPs is that their performance efficiency is largely unknown. In order to address this deficiency, performance evaluation of an oil/grit separator manufactured by Skimpro Technologies in Duluth, Georgia was undertaken in the Hydraulics Laboratory at the Georgia Institute of Technology.

The specific objective of Phase 1 of this study was to measure the removal efficiency of grit and oil in a 1:2 scale model of the Skimpro oil/grit separator for different grit sizes over a realistic range of input flow rates in order to evaluate the existing design and suggest possible design improvements. In Phase 2 of the study, various modifications of the internal baffles of the separator were tested to optimize both oil and grit removal for one grit size and one representative flow rate. For the chosen design, the same grit sizes and range of input flow rates utilized in Phase 1 of the study were repeated in a full series of tests to provide a comparison of the performance of the modified structure to that of the existing design.

The oil/grit separator was operated over a range of expected flow rates to develop removal efficiency vs. surface loading rate relationship curves for oil alone, and for three different grit size distributions. In addition, detailed velocity distributions were measured

inside the oil/grit separator to visualize the flow patterns for different baffle arrangements and to explain differences in oil and grit removal efficiency.

In this report, development of the hydraulic model is discussed in Chapter 2. The resulting Skimpro oil-grit separator model is described, and the experimental procedures are summarized in Chapter 3. Performance results are given in Chapter 4 in terms of the fraction of incoming mass of oil and grit trapped in the separator (trap efficiency) for each size of grit and for oil as a function of surface loading rate. The results are reported and discussed for both Phase 1 and Phase 2 tests of the existing and modified baffle designs, respectively, which are compared in detail to highlight the significant improvements in performance that were achieved. A summary is given in Chapter 5.

CHAPTER 2.

HYDRAULIC MODEL DEVELOPMENT

The hydraulic model similitude in this study was based on requiring equal values of surface loading rate in the model and prototype because this is the primary variable affecting sedimentation rates of discrete particles in ideal settling theory (Peavy et al. 1985). The surface loading rate, or overflow rate, is defined as the flow rate through the separator per unit surface area of the separator. In the case of the oil/grit separator as opposed to large water treatment settling basins, the resulting settling efficiency of grit and floating efficiency of oil are also very dependent on the internal baffle arrangement and the degree of turbulent mixing at the chamber inlets and outlets which means that efficiencies can only be evaluated experimentally. Similitude of the jets issuing from ports in the internal baffles depends on the Reynolds number which remains in the turbulent range for all experiments so that similarity of large-scale eddies responsible for mixing is satisfied. The same fluid and sediment densities as expected in the prototype were used in the model in order to reproduce the buoyancy and settling characteristics of the oil and grit through equality of the density ratios. With similarity of surface loading rates as the primary modeling criterion, Froude number similarity cannot be satisfied exactly. As a result, equivalent heads over the outlet weir are slightly lower in the model than in the prototype, but the primary through-flow dynamics are preserved.

The hydraulic model was constructed at a scale of 1:2. The prototype oil/grit separator is depicted in Figure 2.1. It has a surface area of 50 ft^2 (5 ft by 10 ft) and is subject to design flows that vary somewhat depending on the regulating jurisdiction. For example, one suggested design criterion is to limit the contributing drainage area to 1.0

acre of impervious area. If the peak runoff rate from a 1.0-acre impervious parking lot for the 85th percentile annual rainfall event of 1.2 in. in Georgia is calculated according to methods suggested in the Georgia Stormwater Management Manual (2001), the result is approximately 1.8 cfs, or 0.036 cfs/ft^2 surface loading rate. Gwinnett County in the Atlanta metropolitan area suggests a design loading rate of 0.020 cfs/ft^2 (Gwinnett County Stormwater Design Manual, 2005). The corresponding flow rates in the model for a 2.5 ft x 5.0 ft model surface area (12.5 ft^2) are in the range of 0.25 to 0.45 cfs. To obtain a wide range of settling efficiencies, the tested flow rates in the model were from 0.2 to 0.8 cfs, or surface loading rates of 0.016 to 0.064 cfs/ft^2.

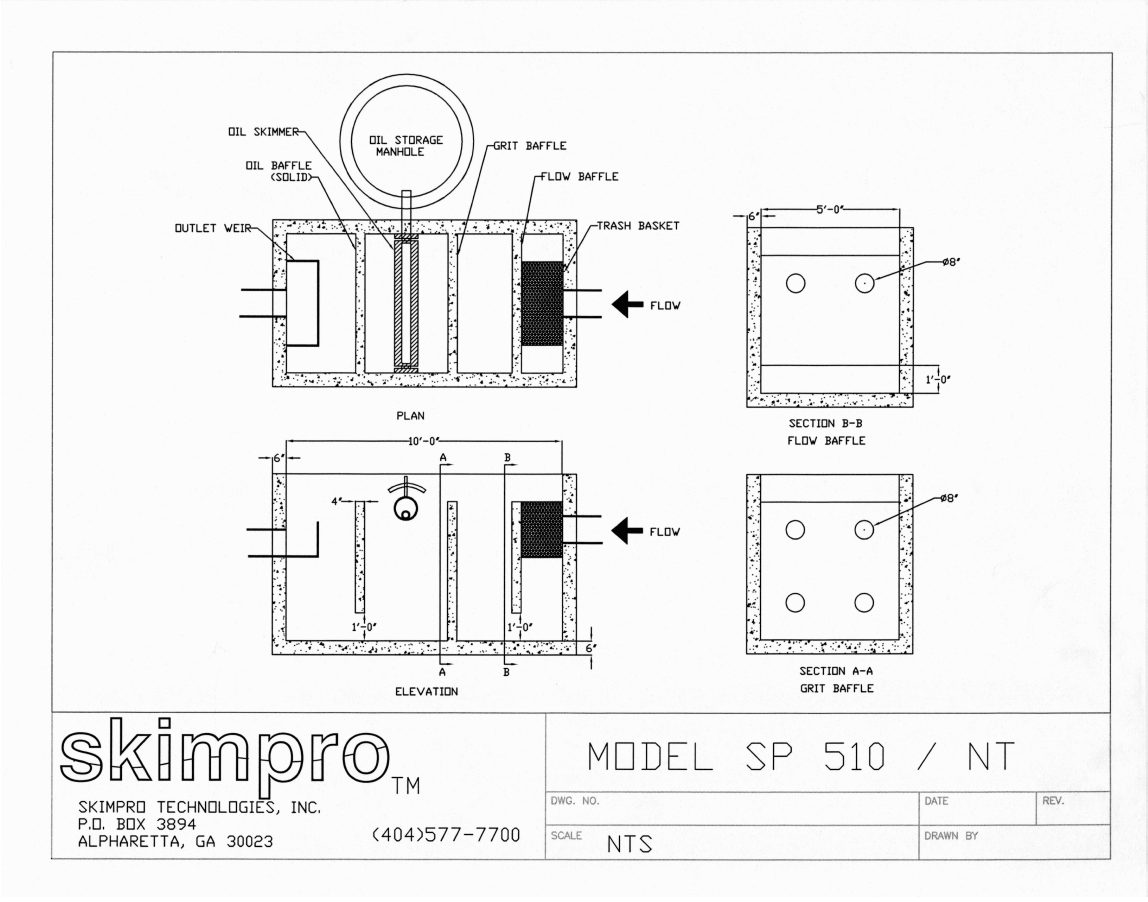

Figure 2.1. Schematic diagram of Skimpro Technologies oil/grit separator.

CHAPTER 3.

EXPERIMENTAL INSTRUMENTATION AND METHODS

3.1 MODEL LAYOUT AND INSTRUMENTATION

The 1:2 scale model was delivered to the hydraulics laboratory at Georgia Tech and installed in a recirculating water system as shown in Figure 3.1. Water discharged from the model through a rectangular flume into an overflow sedimentation tank with a surface area of 50 ft^2 (5 ft x 10 ft). The purpose of the overflow tank was to allow for sedimentation of any sand and surface trapping of oil that exited the Skimpro model. A Goulds fan pump driven by a 3 HP electric motor delivered water from the overflow tank through 6-in. diameter PVC pipe to the upstream end of the Skimpro model. The last 6 ft of pipe immediately upstream of the model was clear PVC to allow for flow visualization (Figure 3.1). A perforated plate was installed in the bend upstream of the clear PVC pipe for flow straightening.

A Marsh-McBirney electromagnetic flow meter was installed in the 6-in. pipe as shown in Figure 3.1, and it was calibrated with a weighing tank. Flow rate was controlled by a gate valve downstream of the flow meter, and measurements of flow rate had an uncertainty of ±0.009 cfs. In the Phase 2 tests, the electromagnetic flow meter was replaced by an orifice meter calibrated with the same weighing tank used for the electromagnetic meter with a similar value of uncertainty.

The sand slurry was maintained in suspension in a mixing tank by continuously stirring with a mixer blade operated with a 0.9 HP motor. The slurry concentration in the

mixing tank was approximately 90,000 mg/L. The slurry was pumped into the inflow pipe by a peristaltic metering pump at a controlled rate at a distance of 4 ft upstream of the separator. The slurry discharged through a 1/4-in. diameter L-shaped tube directed upstream near the pipe centerline to increase mixing (see Figure 3.1). Oil was also fed to the inlet pipe using a separate peristaltic metering pump through a 1/8-in. diameter L-shaped tube pointed upstream and positioned approximately one inch above the bottom of the pipe. The oil was injected at a distance of 6 ft upstream of the model inlet.

Vertical 1/2-in. diameter copper sampling tubes having multiple orifices with diameters of 5/32 in. on 1/2-in. centers were positioned just upstream and downstream of the Skimpro model at the centerline of the inlet pipe and exit channel, respectively. Separate 1 L samples were extracted through the sampling tubes using an ISCO model 6700 programmable pumping sampler.

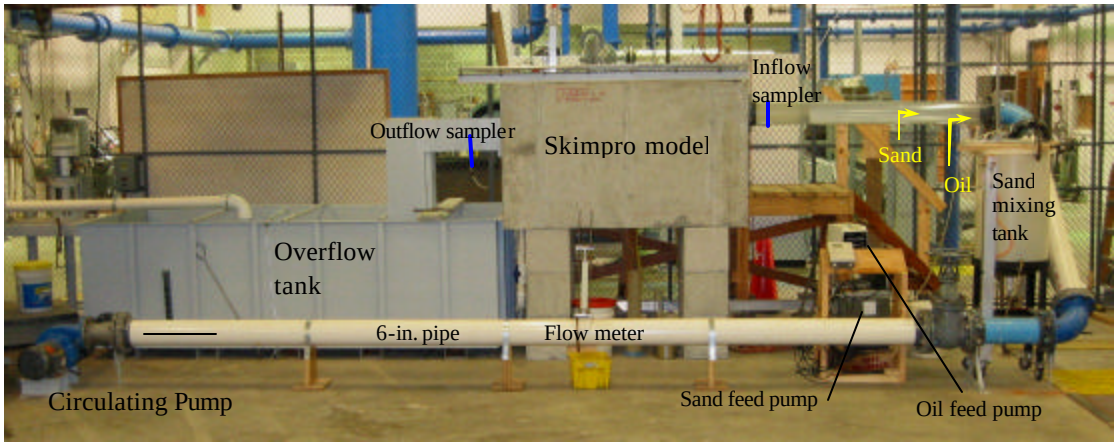

Figure 3.1. Experimental Setup.

Detailed velocity distributions in all three dimensions were measured in the main chamber of the Skimpro oil/grit separator using a SonTek acoustic Doppler velocity

meter (ADV) shown in Figure 3.2 The operation principle of the ADV is based on the Doppler frequency shift. The ADV measures the velocity in the sampling volume located at the intersection of the transmitted and reflected acoustic beams at a distance of 5 cm below the probe transmitter. A short pulse of sound from the transmitter propagates through the water and is reflected in all directions within the sampling volume by sediment particles. Some portion of the reflected pulse travels back along the receiver axis where it is sampled by the ADV and the processing electronics measure the change in frequency. The Doppler frequency shift measured by the receiver is proportional to the velocity of the reflecting particle that is assumed to move with the same velocity as water.

Figure 3.2 Acoustic Doppler velocity meter.

3.2 SAND AND OIL PROPERTIES

Grit in runoff from streets and other paved surfaces can occur in significant concentrations and display a wide size distribution. As reported in ASCE Manual 77 (1992), the EPA Nationwide Urban Runoff Program (NURP) sampled urban runoff from commercial and residential land at 81 sites in 22 cities. The results indicated an average concentration of total suspended solids (TSS) of 239 mg/L with no influence of any

construction site runoff contributions. Wanielista and Yousef (1993) reported particle size distributions of street sweepings from Orlando, FL in which 50 percent of the particles by weight were found in the size range of 0.25 to 0.50 mm. In a separate study of highway runoff in four cities, approximately 80 percent of the size distribution by weight was less than 0.125 mm in size. Obviously, the magnitude and intensity of the rainfall event and other hydrologic variables such as land slope and soil type could be expected to have a large influence on the size of particles entrained and transported by urban runoff.

In this study, relatively uniform sand obtained from Standard Sand and Silica in Lake Wales, FL was utilized as the feed grit. The sand was introduced into the inlet pipe of the separator as a slurry to produce an inflow concentration of approximately 200 – 300 mg/L. The sand consisted of silica as SiO_2, with a specific gravity of 2.65. In order to cover the full range of expected grit sizes in urban runoff, three size distributions as shown in Figure 3.3 were fed to the Skimpro separator in separate tests. Sand A was a medium sand with a median sieve size (d_{50}) of 0.3 mm, while sand B was a fine sand with d_{50} = 0.12 mm. These two sand size distributions were relatively uniform as measured by a geometric standard deviation which is defined by $s_g = (d_{84.1}/d_{15.9})^{0.5}$ where $d_{84.1}$ is the size for which 84.1 percent of a sample is finer by weight, and $d_{15.9}$ represents the 15.9 percent-finer grain size. As shown in Table 3-1, Sand A and Sand B had values of s_g of 1.62 and 1.46, respectively, which is typical of relatively uniform size distributions. A third sand size distribution, referred to as Sand C, was manufactured by mixing equal weights of Sand A and Sand B to provide a more representative nonuniform distribution that might be found in urban runoff. As shown in Table 3-1, Sand C had a median size

(d_{50}) of 0.17 mm and a geometric standard deviation of 1.93. The coefficient of uniformity, C_u, which is defined as d_{60}/d_{10}, is also given in Table 3-1. Sand C had a coefficient of uniformity of 2.6 while Sands A and B had values of 2.1 and 2.2, respectively.

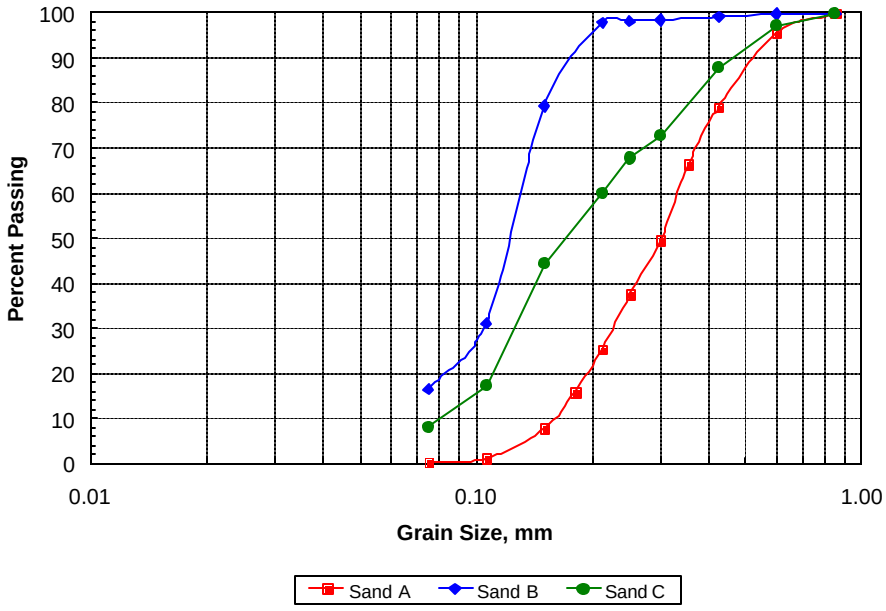

Figure 3.3. Sand size distributions.

Table 3-1. Properties of sand used for grit.

Sand Property	Sand A	Sand B	Sand C
d_{10}, mm	0.159	0.060	0.081
$d_{15.9}$, mm	0.180	0.073	0.102
d_{50}, mm	0.300	0.122	0.166
d_{60}, mm	0.334	0.130	0.210
$d_{84.1}$, mm	0.470	0.155	0.380
s_g	1.62	1.46	1.93
C_u	2.1	2.2	2.6

The oil that was fed to the Skimpro separator was a standard 10W30 motor oil having a specific gravity of 0.871, or a density of 0.871 g/mL. The oil temperature was measured with a thermometer and the specific gravity with a hydrometer for each experimental run.

3.3 INTERNAL BAFFLE DESIGNS AND MODIFICATIONS

Phase 1 studies were completed with a 1:2 scale model of the oil/grit separator as shown schematically in Figure 2.1 with the exception that the oil skimmer pipe located between the grit baffle and the oil baffle was not included. Based on the velocity measurements and trap efficiency results from Phase 1, several internal modifications to the oil/grit separator were tested for Sand C which had the widest distribution of sizes. These tests were all run at a surface loading rate of 0.0375 cfs/ft^2.

The various internal modifications tested in the Phase 2 studies are summarized in Table 3-2 and shown in Figure 3.4. The progression of internal modifications proceeded based on observation of surface flow patterns and trap efficiency performance results for both oil and grit. In Phase 1, the oil skimmer was not included but subsequent tests in Phase 2 (Modification I, referred to as Mod I) showed that it had a measurable effect on oil trap efficiency; however, it was completely submerged and overtopped by the incoming flow from the grit baffle at its initial position. Because of the resulting surface disturbance, the oil skimmer was raised so that only the lower 20 percent of its height was submerged in Mod I-A based on field installation practices for the skimmer. All subsequent tests in Phase 2 used this same position of the oil skimmer. It should also be noted that a vertical extension was added to the top of the grit baffle as shown in Figure

3.4 for both Phase 1 and Phase 2 tests to prevent splashing of the two incoming jet flows over into the next chamber.

In Mod II, the upper two orifices in the grit baffle were replaced by a rectangular notch weir with a crest length as shown in Figure 3.4 (model dimensions) to reduce the surface velocities in the oil removal chamber. Then, in an effort to contain grit in the bottom of the separator, a bottom sill was added as shown in Figure 3.4 in Mod II-A and Mod III. In Mod III, the lower two orifices in the grit baffle were replaced by a 1.5 in. horizontal slot located 3 in. above the floor upstream of the 6-in. high bottom sill. Finally, in Mod 4, the bottom sill was removed and the slot was raised to the original position of the lower pair of orifices at a distance of 6.75 in. above the floor to the lower edge of the slot.

Table 3-2. Internal modifications of oil/grit separator design (model dimensions).

Modification	Description
Phase 1	Existing grit baffle with two pairs of 4-in. orifices; skimmer removed
Phase 2, Mod I	Skimmer added but overtopped
Phase 2, Mod I-A	Skimmer raised to 20% submergence at a surface loading rate of 0.032 cfs/ft^2
Phase 2, Mod II	Skimmer 20% submerged + upper rectangular-notch weir in grit baffle
Phase 2, Mod II-A	Skimmer 20% submerged + weir + 6-in. bottom sill
Phase 2, Mod III	Skimmer 20% submerged + weir +6-in. sill + 1.5 in. slot raised 3 in. above floor
Phase 2, Mod IV	Skimmer 20% submerged + weir + 1.5 in. slot raised 6.75 in. above floor (no sill)

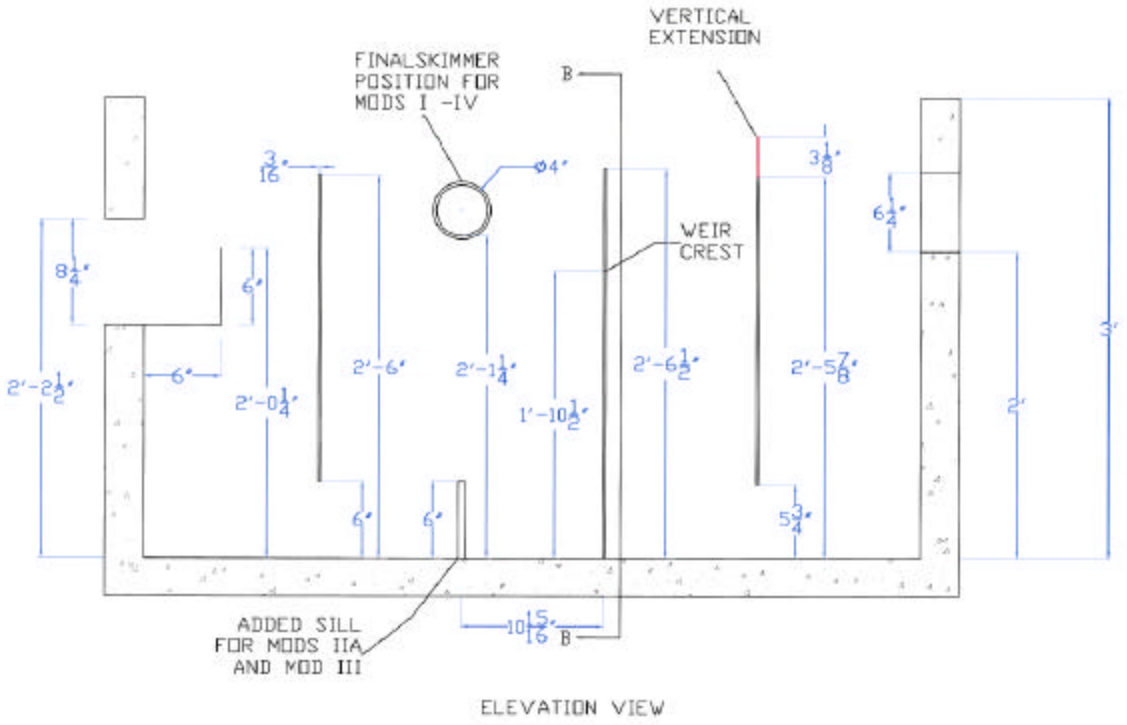

(a) Elevation view showing skimmer, baffle dimensions, and modifications.

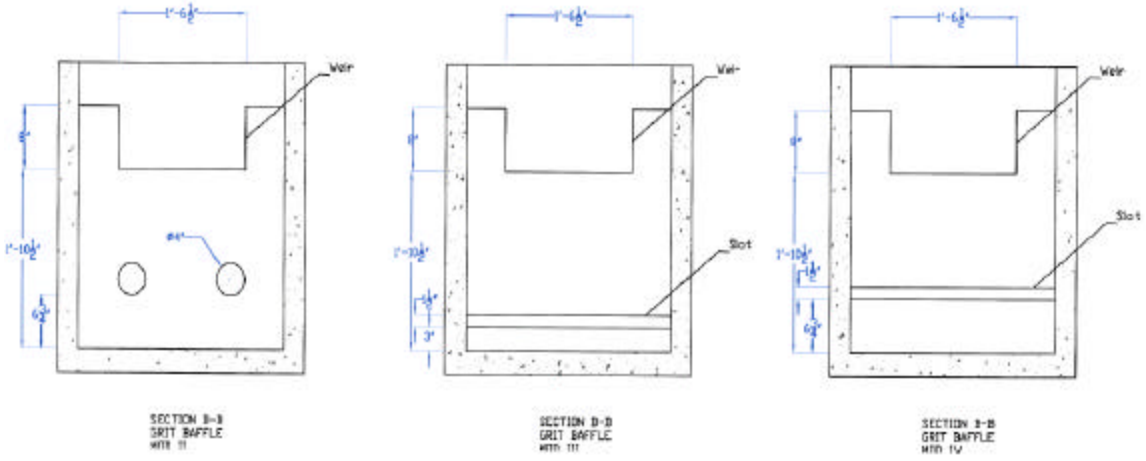

(b) Mod II grit baffle (c) Mod III grit baffle (d) Mod IV grit baffle

Figure 3.4. Skimmer, sill, and internal grit baffle modifications (1:2 model scale; model dimensions in feet and inches).

3.4 EXPERIMENTAL PROCEDURE

3.4.1 Sand Slurry Feed and Trap Efficiency

Prior to each experimental run the overflow sedimentation tank and the Skimpro model were filled with water. The sand slurry was prepared, and mixing was begun to assure a uniform concentration. A preliminary slurry wasting test was conducted to measure the concentration in the mixing tank outlet for decreasing liquid levels as slurry pumping occurred. This test showed that the outlet concentration variability was less than 10 percent from a full tank to a nearly empty tank, but variability was actually much less for each trial because only a portion of the total slurry volume in the tank was needed for a single trial.

An experimental trial was begun by starting the pump and adjusting the gate valve to obtain the desired model flow rate between 0.2 and 0.8 cfs. The water was allowed to circulate for 5 to 10 minutes to come to steady state before beginning the slurry feed pump. The slurry pumping rate was determined such that the fully-mixed concentration in the inlet pipe of the model was approximately 225 mg/L. Based on a separate calibration, the voltage to the slurry pump was adjusted to achieve the desired feed rate. The programmable ISCO sampler was started as soon as the slurry began to enter the inlet pipe of the model. The sampler was programmed to take an inlet sample followed by an outlet sample in alternating fashion at 1-minute intervals for a total of 10 minutes. The total test duration of 10 minutes was chosen in order to assure a minimum of 5 detention times in the Skimpro model. In addition, background samples in the inlet pipe were taken at the beginning and end of the experimental run. All samples were approximately 1 L in volume. At the end of the experimental run, the samples were analyzed for suspended

sediment concentration by filtering and drying according to ASTM standard D 3977-97 (ASTM, 1999).

The trap efficiency of the model was determined by integrating with time the calculated sediment flux into and out of the model over the duration of a test run. Trap efficiency was calculated as the difference between total sediment mass flowing out of the model and total mass flowing into the model divided by the total input mass. Corrections were made to the measured concentrations based on the measured background concentration recirculating through the model, but these corrections were small resulting in less than a 2 percent change in percent of sediment trapped. One test was run at 0.40 cfs in the model in which the total sediment mass collected in the model was carefully siphoned out at the end of the test, and then dried and weighed. Although this was a very tedious and difficult recovery process, the result showed an acceptable mass balance when compared with the calculation of trapped sediment mass based on concentration measurements.

3.4.2 Oil Feed and Recovery

The oil feed tests, with one exception, were conducted separately from the sedimentation tests by feeding only oil to the model. The oil flow rate was set to a constant value and continued for a full 10 minutes such that approximately 3000 g (3.4 L) of oil were fed to the model regardless of the model circulating flow rate. Visual checks of the oil input mode confirmed that the oil entered the inflow pipe in a similar fashion as rising droplets for all tests. The total amount of oil fed to the model was determined by weighing the oil feed reservoir before and after the test. In one series of tests to be described in Chapter 4, both sand and oil were fed to the model simultaneously.

The oil floating on the water surface within the Skimpro model and in the receiving overflow tank was recovered using 18-in. by 18-in. wide by 1/4-in. thick polypropylene oil sorbent pads (McMaster-Carr, Atlanta, GA). The dry weight of the pads was recorded using an electronic balance (0.1 g resolution), and the pads were then used to recover as much free oil as possible. The oil in the pads was extracted by passing each oil-saturated pad through a hand-operated towel ringer (McMaster-Carr, Atlanta, GA). The weight of the recovered oil was determined using a mechanical triple-beam balance (1 g resolution), and a sample of the recovered oil was collected to determine the fraction of water in the oil. The weight of the oil sorbent pads was determined after passing through the hand ringer to account for the residual oil within each pad.

The volume of recovered oil was corrected by subtracting off the volume of water within the oil as estimated by the following procedure. The fraction of water in the recovered oil was estimated using a linear combination of the density of pure water and motor oil:

$$d_{r0} = f_w \times d_w + (1 - f_w) \times d_0 \tag{3.1}$$

where d_{ro} is the measured density of the recovered oil; f_w is the fraction of water in the recovered oil; d_w is the known density of water (0.997 g/mL); and d_o is the measured density of oil (0.871 g/ mL). The fraction of water parameter (f_w) was varied until the calculated density of recovered oil (d_{ro}) was equal to the measured density of recovered oil. The density of recovered oil was measured by filling a 10 mL pycnometer with the recovered oil and recording the mass of the filled pycnometer using an electronic balance (0.001 g resolution).

The trap efficiency of the Skimpro separator was determined as the fraction of oil recovered from the water surface inside the separator at the end of a test relative to the measured total weight of oil added to the system during the test. The total oil recovered from both the separator and the overflow tank satisfied an overall mass balance within ±5 percent.

3.4.3 Concentration of Oil

Water samples were collected in 500 mL glass jars between 9 to 10 minutes after beginning the flow of oil into the system. Two water samples were collected from the Skimpro model: one sample 6 in. from the bottom of the 4th or exit chamber through a 1/4 in. internal dia. (ID) PVC tube and the other sample from water flowing out of the model at the water surface. Two samples were collected from the overflow tank: one sample 6 in. from the bottom of the overflow tank through a 1/4 in. ID PVC tube and the other skimmed from the water within 6 in. of the free water surface. The water samples contained visible droplets of oil and no effort was made to remove the floating oil from the samples.

The hydrocarbons present in each water sample, including the free oil floating on the water surface, were extracted using methods based on EPA SW-846 method 3510C (U.S. EPA, 1996) and Standard Methods method 6410 (APHA, 1998) that involved mixing the water sample with methylene chloride and placing it into a 1 L separatory funnel. The methylene chloride was drained from the funnel and its volume reduced via evaporation to concentrate the hydrocarbons and facilitate detection.

The concentrated methylene chloride extracts were initially analyzed using gas chromatographs (GCs) including a Varian STAR 3400 GC equipped with a Saturn 2000

mass spectrometer (MS) and an Agilent Model 6890 GC equipped with a flame ionization detector (FID). The Varian 3400 GC was equipped with a 30 m by 0.25 mm OD CP-Sil 8 CB low bleed capillary column with the inlet pressure constant at 10 psig using a carrier gas of ultra-high purity (UHP) grade helium to yield a column flow of 1 mL/min at an oven temperature of 60^{o}C. The Agilent 6890 GC was equipped with a 30 m by 0.32 mm OD DB-5 column (Agilent Technologies, Palo Alto, CA). The inlet was operated at 9.93 psig in the split mode (30:1) at 275^{o}C with UHP helium as the carrier gas to produce a constant column flow rate of 2 mL/min. The GC oven temperature was isothermal at 60^{o}C for 1 minute followed by a 20^{o}C/min ramp to 140^{o}C and a 10^{o}C/min ramp to 290^{o}C that was maintained for 20 minutes.

The initial chromatograms were free of elution peaks that could be assigned to individual compounds such as phenanthrene and di-n-butylphthalate, two compounds which were detected by Chen et al. (1994) in water samples that were in equilibrium with water. Instead, the chromatograms were characterized by one broad elution profile that was thought to represent a complex mixture of straight chain aliphatic hydrocarbons that were not separated in the GC column. The concentrated methylene chloride samples were then further treated using methods based on EPA SW846 method 3611B that involved passing the sample through an alumina column (Alltech, Deerfield, IL) and washing the alumina column with hexane, followed by methylene chloride, and then methanol to separate the hydrocarbons into aliphatic, aromatic, and polar fractions. These treated samples were analyzed via GC methods and the aliphatic fraction (hexane fraction) was found to contain the same broad elution profile as in the untreated methylene chloride extract.

The concentration of motor oil in the 500 mL water samples was then determined based on the GC analysis of the aliphatic fraction of the methylene chloride extract. A calibration solution was prepared by adding fresh motor oil to methylene chloride in the concentration range from 2,000 to 50,000 mg/L. These calibration samples were treated using the alumina column method, and the aliphatic fraction was then analyzed to determine GC/FID response to known concentrations of motor oil.

CHAPTER 4.

RESULTS AND DISCUSSION

4.1 VELOCITY MEASUREMENTS

Results for three-dimensional velocity measurements are given in this section to obtain a better understanding of the flow patterns inside the oil/grit separator as affected by various baffle arrangements. The mean flow-through velocity is not sufficient to assess the degree of oil and grit removal because of the highly three-dimensional nature of the velocity field. The velocity field is largely responsible for the resulting trap efficiency achieved by the separator for both oil and grit. Upflow, downflow, separation, entrainment, and recirculation are all turbulent processes that contribute to the degree of mixing and ultimately to the fraction of oil floating on the water surface and grit settled to the bottom of the separator.

4.1.1 Phase 1 Velocity Measurements

Velocity measurements taken in the third chamber of the oil/grit separator (between the grit baffle and oil baffle in Figure 2.1) are shown in Figure 4.1 for a surface loading rate of 0.040 cfs/ft^2, which is approximately the value at which the oil trap efficiency decreased rather sharply in the Phase 1 tests. In Figure 4.1(a), the velocity vectors are shown along the centerline profile of the chamber in the longitudinal direction. (In the remainder of this discussion, the longitudinal axis corresponds to the *x-direction*; the transverse axis is the *y-direction*; and the vertical axis is the *z-direction*).

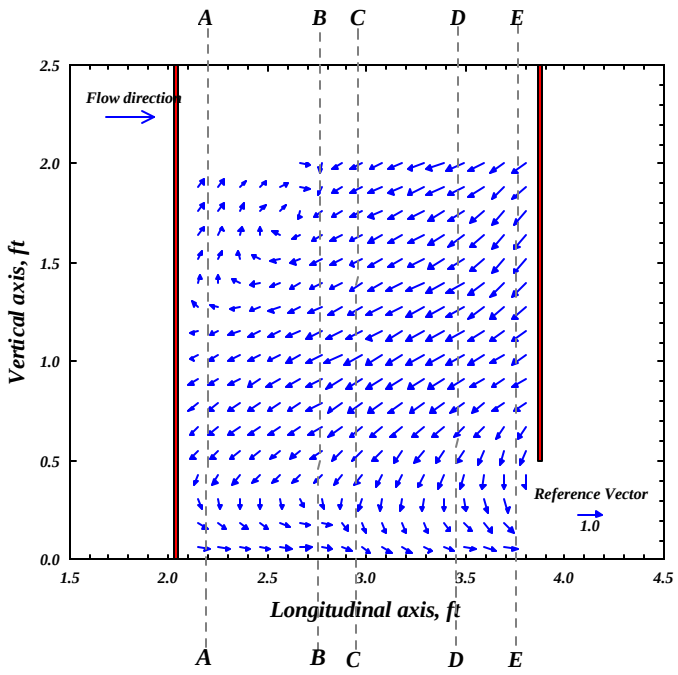

(a) Velocity vectors along centerline (*x-direction)* of oil removal chamber.

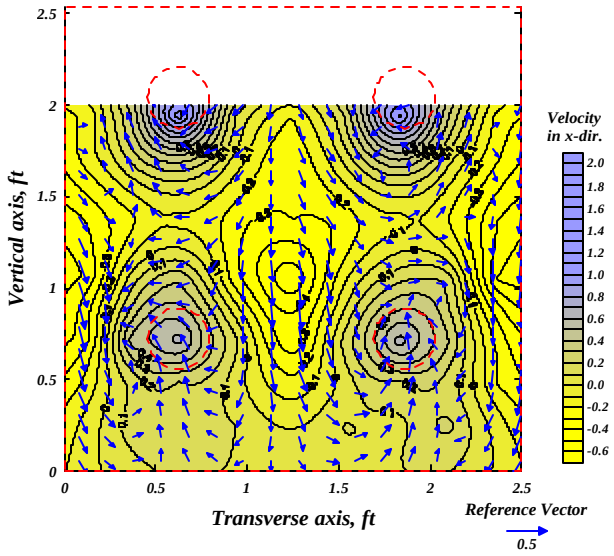

(b) Velocity vectors at section C-C with contours and color scale shown for longitudinal (*x-direction*) velocity components.

Figure 4.1. Velocity field in oil removal chamber for Phase 1 tests without oil skimmer for a surface loading rate of 0.040 cfs/ft^2 (all velocities in ft/sec).

The most notable feature of the velocity field in Figure 4.1(a) is the clockwise separation eddy in the upstream left corner of the chamber caused by the return flow from the blockage due to the oil baffle (just downstream of Section E-E) moving diagonally downward toward the lower left corner and then turning to flow under the oil baffle. The maximum resultant velocity in the diagonal downflow is about 0.8 ft/s at an angle of approximately 30 degrees from the horizontal. The smaller velocity magnitudes exiting under the oil baffle are around 0.3 ft/s.

The velocity vectors at Section C-C in the central cross section of the chamber are shown in Figure 4.1(b). The significant downward velocity components at the centerline are consistent with the profile view in Figure 4.1(a). Downflow also occurs along both walls. Much of the downflow is entrained upward into the lower jets, but a portion also joins the upper jets creating two separate circulations in the upper half of the flow similar to those in the lower half of the flow. Contours of the through-flow velocities in the longitudinal or x-direction are also drawn in Figure 4.1(b) along with a color scale shown at the right side of the figure that indicates velocity magnitude. The maximum return longitudinal velocity (negative x-direction) is approximately -0.6 ft/s near the center of the cross section, while the maximum longitudinal jet velocities at this cross section are about 1.2 ft/s for the upper jets and 0.65 ft/ s for the lower jets. It is likely that the mismatch in velocity magnitudes between the upper and lower jets and the rather large upper jet velocities contribute to the relative performance efficiency of the separator for removing oil vs. grit. The result of the jet impact with the downstream oil baffle is a recirculating flow with vertical and horizontal velocity components that negatively impact both sedimentation and oil retention.

4.1.2 Phase 2 Velocity Measurements

Velocity vectors are shown in Figure 4.2 for Modification I-A (Mod I-A) in which the oil skimmer was placed in the oil removal chamber of the separator with a submergence of approximately 20 percent. The oil and grit baffle plates were unchanged from Phase 1 in this modification.

In comparing Figures 4.1(a) and 4.2(a), it can be observed that the recirculating eddy in the upper left corner of the chamber expanded in the streamwise direction due to the presence of the oil skimmer and disruption of the jet flows on either side of the centerline. The maximum resultant velocity in the diagonal downflow is about 0.7 ft/s at an angle of approximately 30 degrees to the horizontal, and the smaller horizontal velocities under the oil baffle are about 0.25 ft/s. These velocity values are only slightly less than the corresponding values in Figure 4.1(a) without the skimmer.

The velocity vectors shown for Section C-C upstream of the skimmer in Figure 4.2(b) display a split in direction with respect to a horizontal line located at a z value of about 1.0 ft. Upward flow occurs above that line and downward flow below it due to entrainment into the upper and lower jet flows, respectively. Downstream of the skimmer at Section D-D, the velocity vectors shown in Figure 4.2(c) form a pattern very similar to those observed in Figure 4.1(b) for Phase 1. There is a vertical downflow at the centerline and walls with secondary circulations created by entrainment into the jet flows.

At Section C-C upstream of the skimmer shown in Figure 4.2(b), the maximum longitudinal jet velocities are approximately 1.3 ft/s in the lower jets and 1.5 ft/s in the upper jets. In Figure 4.2(c), just downstream of the skimmer, the maximum longitudinal

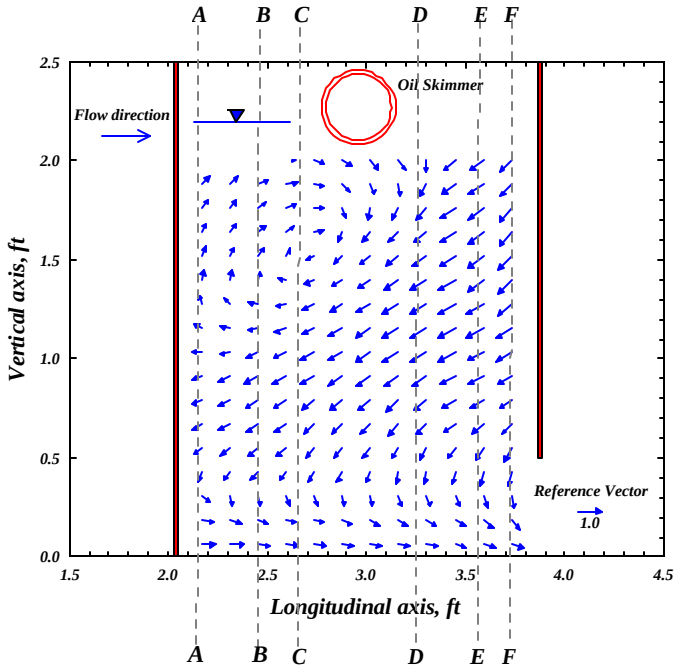

(a) Velocity vectors along centerline (*x-direction)* of oil removal chamber (Mod I-A).

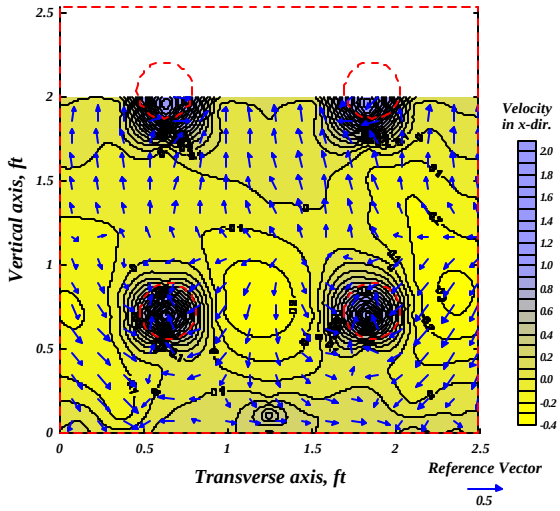

(b) Velocity vectors at section C-C with contours and color scale shown for *x-direction* velocity (Mod I-A).

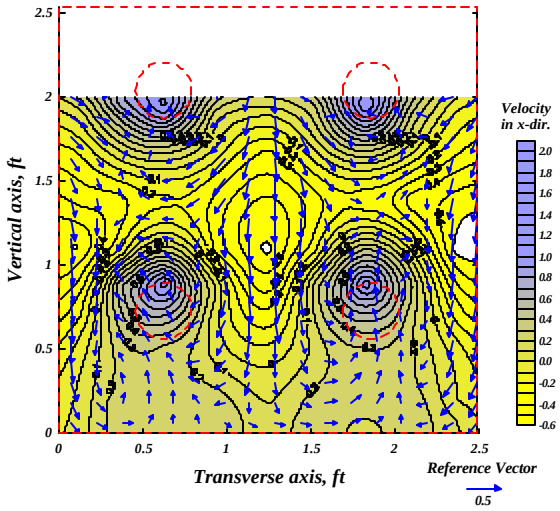

(c) Velocity vectors at section D-D with contours and color scale shown for *x-direction* velocity (Mod I-A).

Figure 4.2. Velocity field in oil removal chamber for Mod I-A tests with oil skimmer for a surface loading rate of 0.040 cfs/ft^2 (all velocities in ft/sec).

jet velocities are about 1.1 ft/s in the lower jets and 1.2 ft/s in the upper jets. In comparison to Figure 4.1(b), the upper and lower jet velocities in Figure 4.2(b) and (c) are more nearly equal to each other due to the presence of the skimmer.

In Figure 4.3 the velocity vectors are shown for Modification IV (Mod IV) in which the upper orifices in the grit baffle have been replaced by a rectangular-notch weir, and a rectangular slot has been cut in the grit baffle at the former location of the lower orifices in Phase 1. The skimmer remains in place as in Mod I-A. (Refer to Table 3-2 and Figure 3.4). The centerline profile of velocity vectors shown in Figure 4.3(a) is dramatically different than for the previous grit baffle configurations shown in Figures 4.1 and 4.2. There is a persistent longitudinal streamwise flow (positive *x*-direction) near the water surface that is largely unchanged in direction by the oil skimmer. Furthermore, there is no diagonally reverse downward flow for Mod IV; instead there is an upward entrainment component attracted by the weir flow with most of the downflow located at the end of the chamber. The longitudinal, horizontal components (*x*-direction) of the velocities under the oil baffle are very small with values of about 0.10 to 0.18 ft/s which are less than the Phase 1 and Mod I-A values.

The velocity vectors for Section C-C just upstream of the oil skimmer are shown in Figure 4.3(b). The introduction of the upper weir and lower slot produces a more uniform longitudinal velocity distribution across the cross section in comparison with the flow patterns in Figures 4.1 and 4.2. Upflow occurs upstream of the skimmer over most of the central width of the chamber and downflow exists only near the walls. The longitudinal, horizontal velocities (*x*-component) are also much different with a positive

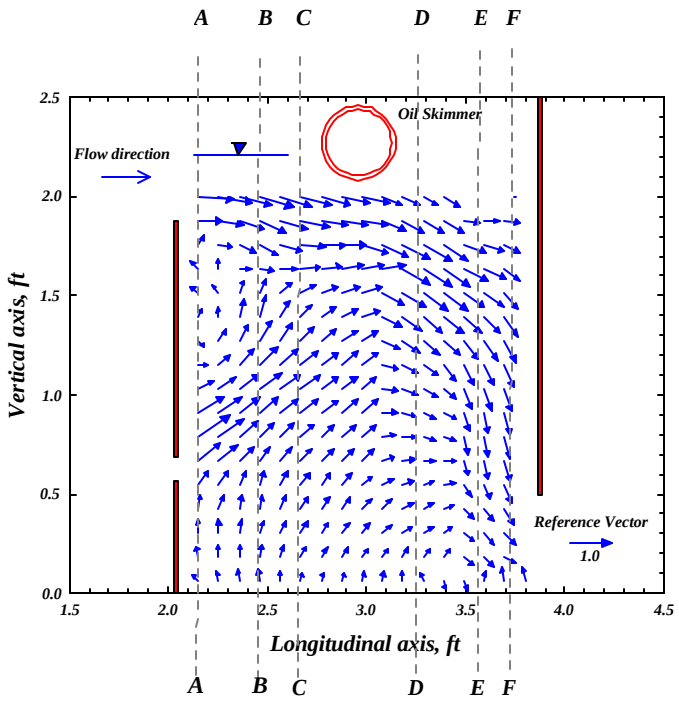

(a) Velocity vectors along centerline (*x-direction)* of oil removal chamber (Mod IV).

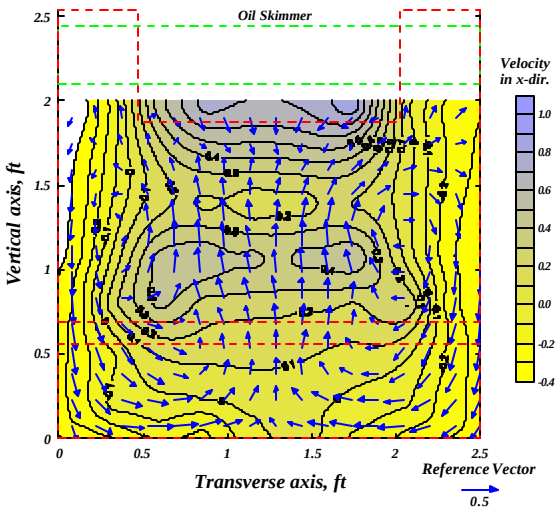

(b) Velocity vectors at section C-C with contours and color scale shown for *x-direction* velocity (Mod IV).

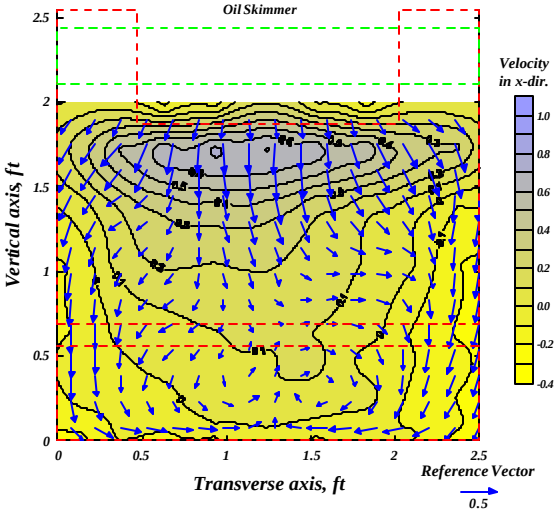

(c) Velocity vectors at section D-D with contours and color scale shown for *x-direction* velocity (Mod IV).

Figure 4.3. Velocity field in oil removal chamber for Mod IV tests with oil skimmer for a surface loading rate of 0.040 cfs/ft^2 (all velocities in ft/sec).

x-direction over most of the cross section. The maximum values are around 0.4 ft/s in the central portion of the cross section and 1.0 ft/s in the weir flow in comparison to 1.5 ft/s in the upper jets in Mod I-A. The return *x*-component velocities are confined to a region near the vertical walls and the bottom with a maximum magnitude of about −0.3 ft/s.

In Figure 4.3(c) just downstream of the oil skimmer at Section D-D, it can be observed that the secondary velocity components in the vertical z-direction are predominantly downward in contrast to those in Figure 4.3(b) upstream of the skimmer. In addition, the two positive *x*-component velocity regions of Figure 4.3(b) due to the weir and the slot have merged into a single one in Figure 4.3(c) downstream of the skimmer with a maximum magnitude of about 0.7 ft/s.

4.1.3 Summary of Velocity Measurements

The resulting three-dimensional flow field that can be deduced from Figures 4.1 (Phase 1) and 4.2 (Phase 2, Mod I-A) leads to the conclusion that the oil skimmer has some effect on the flow field, but it is still dominated by relatively large vertical and horizontal velocity components due to jet impact against the oil baffle and entrainment into the four separate jet flows from the orifices in the grit baffle. The strategy employed in the grit baffle configuration of Mod IV of reducing the flow concentration with an upper rectangular weir and a lower rectangular slot significantly reduces horizontal velocity components and recirculations as shown in Figure 4.3. As a result, oil is more likely to accumulate near the water surface in the oil removal chamber, and horizontal outflow velocities near the bottom of the chamber are smaller in magnitude, and thus less likely to carry grit out of the separator.

4.2 PHASE 1 GRIT AND OIL REMOVAL RESULTS

4.2.1 Grit Trap Efficiency

Trap efficiency curves for the three sand sizes tested as grit and for the motor oil are shown in Figure 4.4. For the coarsest sand (Sand A) with a median grain size of d_{50} = 0.30 mm, the trap efficiency is above 80 percent for surface loading rates less than 0.040 cfs/ft^2, which is slightly greater than the maximum design loading rate of 0.036 cfs/ft^2 based on a contributing drainage basin of one acre of impervious area and a rainfall of 1.2 in. according to Georgia standards as discussed previously in Chapter 2 of this report. The maximum trap efficiency for Sand A is 96 percent at the lowest surface loading rate tested of 0.016 cfs/ft^2 which is slightly less than the Gwinnett County suggested design loading rate of 0.020 cfs/ft^2. Corresponding trap efficiencies at this lowest tested loading rate are 80 percent for Sand B (d_{50} = 0.12 mm) and 83 percent for Sand C (d_{50} = 0.17 mm). At a suggested maximum design loading rate of 0.036 cfs/ft^2, the trap efficiency exceeds 40 percent for all three sand sizes tested.

The suggested performance criterion for total suspended solids (TSS) removal by oil/grit separators is 40 percent (Georgia Stormwater Management Manual, 2001), so the Skimpro separator is considerably more than adequate at a maximum design loading rate of 0.036 cfs/ft^2, and in fact produces trap efficiencies for TSS removal comparable to sedimentation ponds (≥80 percent) at a design loading rate of 0.016 cfs/ft^2 for all three sand sizes tested. The trap efficiency becomes unacceptable (<40 percent) for fine sand (Sand B) for loading rates in excess of approximately 0.040 cfs/ft^2 which is not unexpected based on the measured velocity fields shown previously in Figure 4.1.

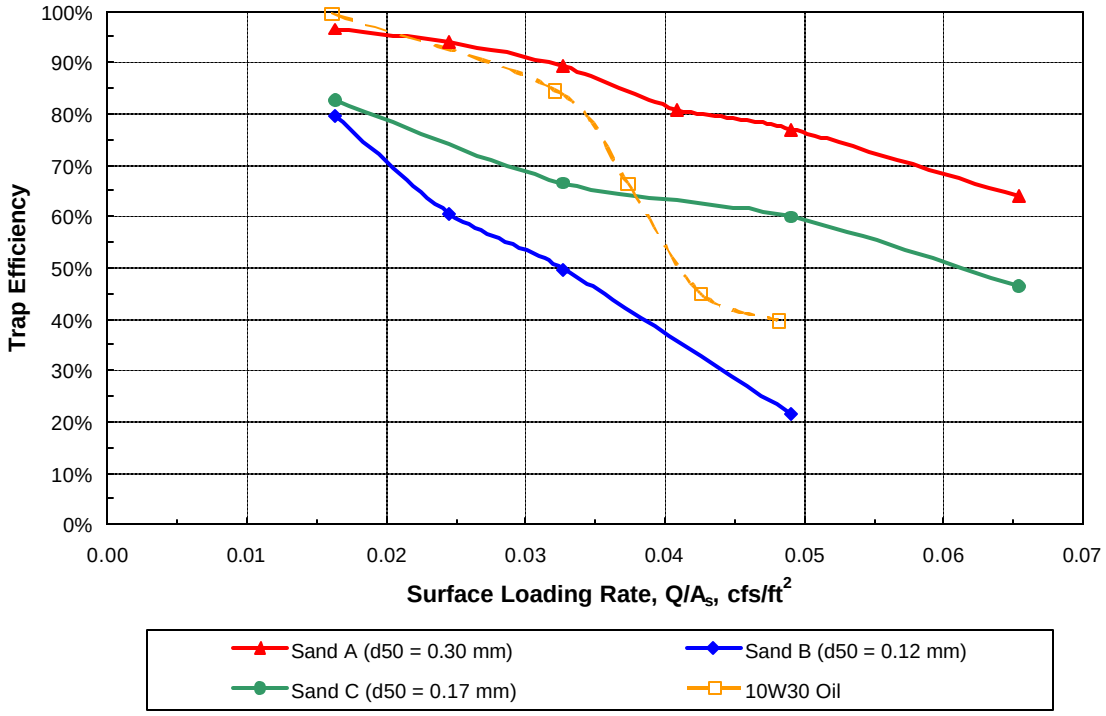

Figure 4.4. Phase 1 results for trap efficiency of grit and oil.

4.2.2 Oil Trap Efficiency

The oil trap efficiency is also shown in Figure 4.4 for comparison with the values obtained for sand. It is interesting to note that the oil trap efficiency is greater than 80 percent at a surface loading rate of 0.032 cfs/ft^2 and is comparable with TSS trap efficiency for the coarse sand (Sand A) for surface loading rates less than this value. The oil trap efficiency drops very rapidly for loading rates greater than 0.032 cfs/ft^2, although it does not fall below 40 percent for rates as high as nearly 0.050 cfs/ft^2. These results are for the case of oil feed alone without sediment feed to the separator. One test run was made at a loading rate of 0.037 cfs/ft^2 with both oil and sand (Sand C) fed simultaneously

to the separator. This trial test suggested that further combined tests with simultaneous feeding of both oil and grit might be of interest. These tests were run in Phase 2 and the results are reported in Section 4.5.

4.2.3 Oil Concentration

Table 4-1 gives the concentration of motor oil in the water samples collected from the Skimpro experiments. These concentrations represent the total amount of motor oil found in the 500 mL water samples, both dissolved in water and floating on the water surface, so it is important to note that they do not represent typical pollutant concentrations reported as either dissolved or suspended. Water was at the maximum solubility limit (i.e., saturated) in all trials since separate-phase oil was present in all the water samples.

Table 4-1. Concentration of motor oil in water samples (mg oil/L)

	Skimpro separator		Overflow tank	
Trial number (cfs/ft^2)	Outflow Surface	Bottom of 4^{th} Chamber	Water Surface	Bottom
1	NC[1]	NC	NC	NC
2	NC	NC	NC	NC
3 (0.016)	NC	85	NC	NC
4 (0.042)	241	219	710	84
5 (0.042)	242	463	491	167
6 (0.037)	314	322	669	122
7 (0.037/with sand feed)	218	267	561	111

[1]NC: not collected

Separate-phase oil was found in water samples collected from within the Skimpro 1:2 scale model and from the overflow tank. The presence of separate-phase oil in water

samples collected from near the bottom of the 4th chamber in the Skimpro model was not anticipated. This result suggests that oil entering the Skimpro model forms droplets that are small enough to pass through the oil skimmer chambers, flow under the oil baffle, and exit the Skimpro model. These small oil droplets were also visible in the overflow tank and evident in water samples collected from the bottom of the tank. Thus once formed, these droplets are stable and remain in the water column long enough to pass through the Skimpro model and resist flocculation in the overflow tank.

Repeatable results for the outflow concentration of oil at the water surface in the Skimpro separator were obtained for experimental trials 4 and 5 at the same loading rate; however, the overflow tank concentrations show some variability likely due to the heterogeneous mixture of oil droplets and water.

4.3 RESULTS OF PHASE 2 TRIALS TO IMPROVE TRAP EFFICIENCY

A series of experimental trials was run with different modifications of the grit baffle in the Skimpro separator in order to improve the overall performance as measured by trap efficiency. The baffle modifications were summarized previously in Table 3-2 and Figure 3.4. All trials were run at the same surface loading rate of 0.0375 cfs/ft^2 which is in the upper range of acceptable design surface loading rates. The grit used in each of these experimental trials was Sand C (d_{50} = 0.17 mm), which represented a nonuniform size distribution obtained by mixing Sand A and Sand B (see Figure 3.3).

The results for trap efficiency for both grit and oil for Phase 1 and for all of the Phase 2 modifications of the grit baffle are given in Table 4-2 for a surface loading rate of 0.0375 cfs/ft^2 with Sand C used as grit.

Table 4-2. Phase 1 and Phase 2 trap efficiencies in percent for oil and grit at surface loading rate of 0.0375 cfs/ft^2.

Contaminant	Phase 1*	Phase 2** Mod. I	Mod. I-A	Mod. II	Mod. II-A	Mod. III	Mod. IV
Oil	67	52	59	71	63	79	78***
Grit – Sand C (d_{50}=0.17 mm)	64	76	72	62	53	51	69

**Phase 1 –- no skimmer, 2 pairs of 4 in. orifices*

***Phase 2*

Mod. I –- skimmer added but overtopped

Mod. I-A –- skimmer 20% submerged

Mod. II –- skimmer + upper weir

Mod. II-A –- skimmer +upper weir + 6 in. sill

Mod. III –- skimmer + upper weir + 6 in. sill + lower 1.5 in. slot raised 3 in. above floor

Mod. IV –- skimmer + upper weir + lower 1.5 in. slot raised 6.75 in. above floor (no sill)

****Interpolated from Figure 4.5*

The values given for trap efficiency for both oil and grit for Modification I (Mod I) in Table 4-2 are not representative with respect to the position of the oil skimmer relative to the free surface of the water as it is currently installed in practice. This was rectified in Mod I-A in which the skimmer was positioned based on the past installation experience of Skimpro Technologies. The resulting trap efficiencies for Mod I-A decreased for oil and increased for grit compared to the Phase 1 results with no skimmer in place. The subsequent changes in the grit baffle described next and summarized in Table 4-2 had the objective of increasing both oil and grit efficiency by obtaining a better balance between upper and lower velocities in the oil removal chamber and reducing the magnitude of velocities throughout the chamber.

The change in Mod II consisted of replacing the two upper orifices in the grit baffle with a rectangular-notch weir because the velocity measurements revealed relatively high velocities due to the jets from the orifices as discussed in Section 4.1.2.

While this modification increased the oil trap efficiency to 71 percent, the grit efficiency decreased in comparison to Mod I-A as shown in Table 4-2.

Next in Mod II-A, a sill across the bottom of the oil removal chamber was placed beneath the skimmer in an attempt to reduce the sweeping out of grit underneath the oil baffle plate by the jet flows from the two lower orifices. This modification not only reduced the oil trap efficiency but decreased the grit trap efficiency even more in comparison to Mod II as shown in Table 4-2. This may have been due to an imbalance in upper and lower velocities caused by the combination of the lower jets and the sill.

In order to eliminate the undesirable interaction of the lower jet velocities and the sill, the lower circular jets were replaced by a rectangular slot that extended across the full width of the oil removal chamber, while the sill was left in place in Mod III. This modification also failed because it resulted in the lowest grit efficiency of any previous modification although there was a significant increase in oil trap efficiency as seen in Table 4-2.

The final modification (Mod IV) consisted of removing the bottom sill and raising the lower rectangular slot in the grit baffle higher off the bottom so that it would be higher than the sluice opening under the oil baffle. This modification maintained the high oil efficiency of Mod III, with a value of about 78 percent, and also reversed the trend of decreasing grit trap efficiencies with a new value of 69 percent. As shown in Table 4-2, this latter value for grit trap efficiency exceeded the Phase 1 results by five percent in trap efficiency while remaining only three percent below the grit trap efficiency obtained with Mod I-A for the properly positioned oil skimmer.

Oil concentrations measured in water samples taken at the water surface and the bottom of the oil/grit separator near its outlet are given in Table 4-3. In addition, concentrations at the surface and bottom of the overflow tank are shown in Table 4-3. It is clear from these data that modifications which increased the oil trap efficiency also significantly reduced the oil concentrations near the outlet of the Skimpro separator. The oil concentration at the outflow surface decreased from 314 mg/L, for example, for Phase 1 to 25 mg/L for Mod IV.

Table 4-3. Concentration of motor oil in water samples for a surface loading rate of 0.0375 cfs/ft^2 (mg oil/L)

	Skimpro separator		Overflow tank	
Baffle Configuration	Outflow Surface	Bottom of 4th Chamber	Water Surface	Bottom
Phase 1 (no skimmer)	314	322	669	122
Phase 2, Mod I-A	119	179	174	33
Phase 2, Mod II	54	100	693	9
Phase 2, Mod II-A	105	113	1165	24
Phase 2, Mod III	65	40	464	6
Phase 2, Mod IV	25	30	131	15

Based on the results presented in this section, it was jointly decided between Skimpro Technologies and Georgia Tech to proceed with complete testing of the performance of Mod IV because it best achieved high trap efficiencies for both oil and grit.

4.4 RESULTS FOR GRIT REMOVAL BY SEPARATOR WITH MODIFICATION IV

Grit removal efficiency for Mod IV of the grit baffle is shown in Figure 4.5 as a function of surface loading rate on the oil/grit separator for all three grit size distributions referred to as Sands A, B, and C (see Figure 3.3).

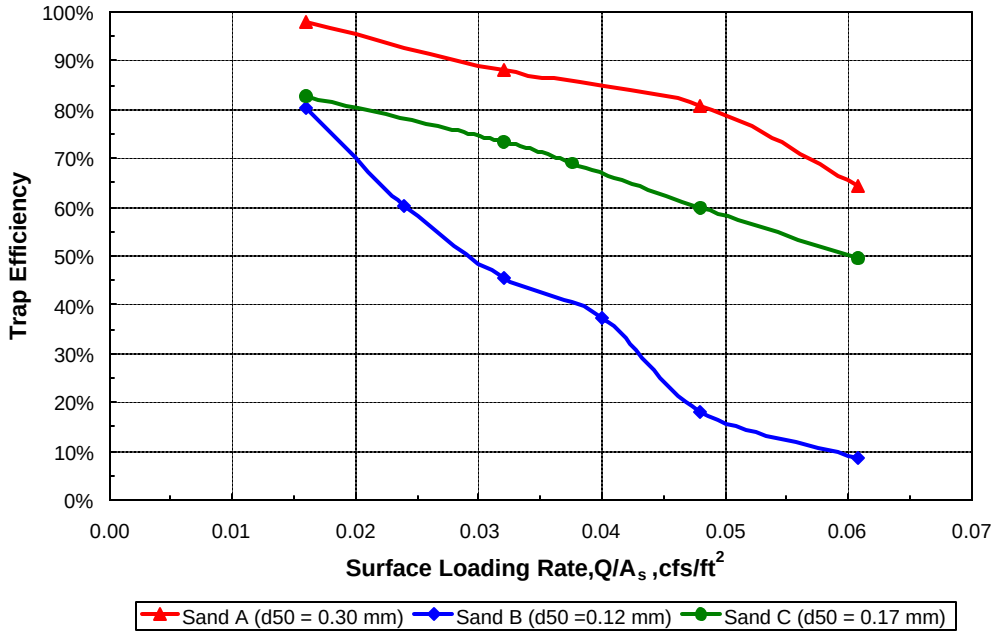

Figure 4.5. Phase 2-Mod IV results for trap efficiency of grit.

As in the case of Phase 1 results, the Phase 2-Mod IV oil/grit separator achieved greater than 80 percent grit removal efficiency for all three grit size distributions at the lowest tested surface loading rate of 0.016 cfs/ft^2, which is only slightly less than the Gwinnett County (2005) suggested loading rate of 0.020 cfs/ft^2. At the calculated maximum surface loading rate of 0.036 cfs/ft^2 according to the Georgia Stormwater Manual (2001), the grit trap efficiency exceeded 40 percent for all three grit size distributions. In fact, the Skimpro separator exceeded 40 percent grit removal even at

surface loading rates as high as 0.060 cfs/ft^2 for Sand A and Sand C. This would correspond to peak runoff discharges of approximately 3.0 cfs for a prototype separator with surface dimensions of 5 ft by 10 ft.

4.5 RESULTS FOR OIL REMOVAL BY SEPARATOR WITH MODIFICATION IV

Results for oil trap efficiency (relative volume of oil trapped in Skimpro separator) for the Phase 2-Mod IV configuration of the grit baffle are shown in Figure 4.6. The relative volume of oil measured in the overflow tank and the relative total volume of oil recovered are also given in Figure 4.6. The experimental mass balance for the oil is very good, with a maximum deviation from 100 percent of only three percent.

It can be observed in Figure 4.6 that the oil trap efficiency is greater than or equal to 80 percent for surface loading rates up to the maximum recommended loading rate of 0.036 cfs/ft^2. This is a very significant improvement in oil trap efficiency in comparison to the Phase 1 results as shown in Figure 4.6. The oil trap efficiencies shown for Mod IV are elevated above those for Phase 1 over an extended range of surface loading rates up to values of nearly 0.06 cfs/ft^2. At a surface loading rate of 0.042 cfs/ft^2, for example, the oil trap efficiency increased from approximately 45 percent in Phase 1 to 72 percent for Mod IV in Phase 2 which is an increase by a factor of 1.6. The sudden drop in oil efficiency observed in the Phase 1 results at this surface loading rate was eliminated by the Mod IV grit baffle design. Oil trap efficiency was greater than 40 percent for surface loading rates as high as 0.06 cfs/ft^2 which extended the effective flow operating range of the Skimpro separator from 0.048 cfs/ft^2 in Phase 1 to 0.06 cfs/ft^2 in Mod IV. This improvement represents a relative increase in allowable maximum flow of approximately 25 percent while maintaining an oil trap efficiency of at least 40 percent.

For the experimental runs that included simultaneous inflow of oil and grit (Sand C) to the Skimpro separator, the oil removal efficiency was about the same as for the case of oil inflow alone as shown in Figure 4.6. Apparently, insufficient mixing of the oil and grit occurred for any measurable adherence or adsorption of oil to the sand grains in the Mod IV design.

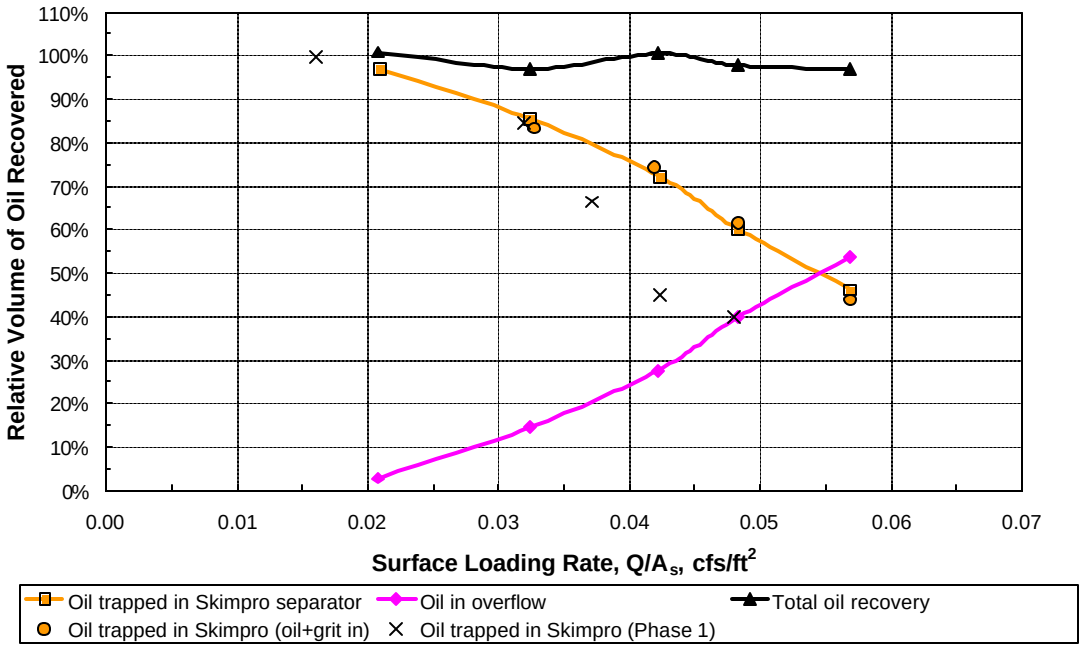

Figure 4.6. Phase 2-Mod IV results for trap efficiency of oil.

4.6 COMPARISON OF PHASE 1 AND PHASE 2-MOD IV RESULTS

Results for both grit and oil trap efficiency are compared for the Phase 1 and Phase 2-Mod IV experiments in Figure 4.7. The dramatic improvement in oil trap efficiency to achieve acceptable oil removal rates at much higher surface loading rates for Mod IV in comparison to Phase 1 results is apparent. The comparison of grit trap efficiency data in

Figure 4.7 shows that the Mod IV and Phase 1 results are comparable. This objective was achieved only after several attempts at modifying the lower openings in the grit baffle to work in concert with the improved oil trap efficiency afforded by the upper rectangular weir.

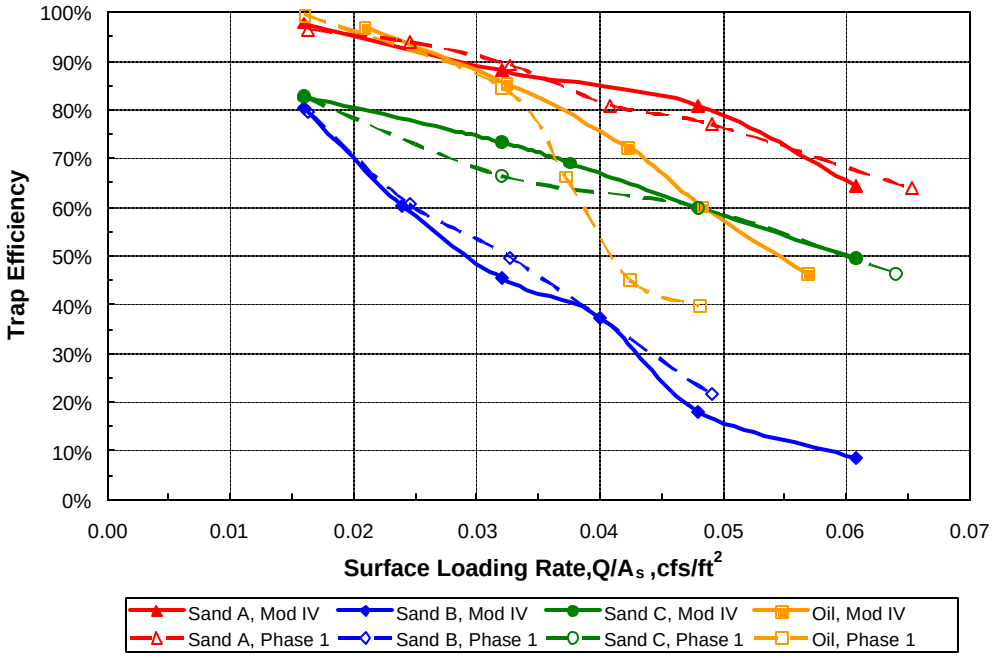

Figure 4.7. Comparison of Phase 1 and Mod IV results for trap efficiency of oil and grit.

CHAPTER 5.

SUMMARY AND CONCLUSIONS

Experimental tests of a 1:2 scale model of an oil/grit separator designed by Skimpro Technologies of Duluth, Georgia were conducted in the Hydraulics Laboratory at the Georgia Institute of Technology. A recirculation system with a large sedimentation tank downstream of the separator was set up so that oil and grit could be fed continuously to the separator through the inlet pipe and trap efficiencies could be measured. Three different sands with different size distributions were used as grit, and 10W30 motor oil was utilized as a representative hydrocarbon in urban runoff from parking lots. The sand concentrations were measured upstream and downstream of the separator in 1 L samples obtained with a programmable pumping sampler. From the measured inflow and outflow concentrations and the measured circulating flow rate, inflow and outflow fluxes were computed and integrated with respect to time to determine the trap efficiency for sand. Oil trap efficiency was measured by recovering the oil in the separator and the overflow tank at the end of an experimental trial and comparing the results with the measured total weight of oil fed to the separator during the experiment. Surface loading rates of water circulated through the separator varied from 0.016 cfs/ft^2 to 0.064 cfs/ft^2.

Velocities measured in three dimensions in the main chamber of the separator showed a recirculating flow pattern set up by the concentrated orifice flow from the grit baffle that impacted the downstream oil baffle for the Phase 1 configuration of the grit baffle without the oil skimmer. Measured velocities at the maximum loading rate were somewhat higher than desirable which negatively impacted the oil and grit trap

efficiencies. As a result, Phase 2 of the study was undertaken to determine what modifications to the oil/grit separator could be made to maximize trap efficiency.

Addition of the oil skimmer to the main oil removal chamber in Mod I-A affected the velocity pattern upstream of the skimmer but had much less effect downstream of the skimmer. The final selected modification of the grit baffle (Mod IV) resulted in a much less concentrated velocity field with a very different flow pattern in the oil removal chamber. The Mod I-A grit baffle plate with 4 orifices produced large vertical downflow velocity components at the centerline and walls of the oil removal chamber accompanied by secondary circulations in the vertical cross section created by entrainment into the jet flows. To alleviate this flow concentration, the Mod IV baffle plate reduced the longitudinal velocity components by spreading the flow laterally across the chamber width through an upper rectangular weir and a lower rectangular slot. As a result, vertical velocity components were smaller and directed upward toward the weir flow across the entire chamber. Horizontal outflow velocities near the bottom of the chamber were also smaller in magnitude. The performance response was an enhanced accumulation of oil at the water surface in the oil removal chamber without hindering grit settling and retention at the bottom of the chamber.

In the Phase 1 tests, the oil trap efficiency exceeded 80 percent at a surface loading rate of 0.032 cfs/ft^2 and was comparable with grit trap efficiency for the coarse sand (Sand A) for surface loading rates less than this value. However, the oil trap efficiency declined very rapidly for surface loading rates greater than 0.032 cfs/ft^2 in the Phase 1 experiments. This significant deficiency in performance of the oil/grit separator was remedied by Mod IV in the Phase 2 tests through alteration of the internal velocity

distributions as just described. The oil trap efficiencies for Mod IV were elevated above those for Phase 1 over an extended range of surface loading rates up to values of nearly 0.06 cfs/ft^2. At a surface loading rate of 0.042 cfs/ft^2, for example, the oil trap efficiency increased from approximately 45 percent in Phase 1 to 72 percent for Mod IV in Phase 2 which is an increase by a factor of 1.6. In terms of maintaining a minimum oil trap efficiency of 40 percent, the Mod IV design extended maximum allowable flow rates by 25 percent in comparison to the Phase 1 results. The Mod IV design also significantly reduced the oil concentrations near the outlet of the Skimpro separator. The oil concentration at the outflow surface in the separator decreased from 314 mg/L, for example, for Phase 1 to 25 mg/L for Mod IV.

Trap efficiencies for the three different sands with median sizes of 0.12 mm, 0.17 mm, and 0.30 mm were greater than 80 percent at a surface loading rate of 0.016 cfs/ft^2 for both Phase 1 and Mod IV results. At a suggested maximum design loading rate of 0.036 cfs/ft^2, the grit trap efficiency exceeded 40 percent for all three sand sizes tested in the Phase 1 and the Mod IV configurations. This performance meets or exceeds current suggested design guidelines for oil/grit separators. In other words, the improved oil trap efficiency of the Mod IV design was achieved without reduction of the very high grit trap efficiencies measured in Phase 1. Several modifications were required to determine the final configuration, which balanced the very different flow-pattern requirements for oil vs. grit removal to obtain high values for both over a wide operating range of flow rates.

For the experimental runs that included simultaneous inflow of oil and grit (Sand C) to Mod IV of the Skimpro separator, the oil removal efficiency was about the same as

for the case of oil inflow alone. Apparently, insufficient mixing of the oil and grit occurred for any measurable adsorption or adherence of oil to the sand.

In conclusion, these test results demonstrated successful improvement of the Skimpro oil/grit separator because its performance was shown to be more robust for oil and grit removal over a wider range of flow rates. This is especially important for application of the separator to urban runoff quality control in the case of storms that occur with high frequency. In order to meet present and future water quality regulations for stormwater runoff from industrial and commercial impervious surfaces, oil/grit separators that have been optimized for both oil and grit removal as in this study have an important role to play in reducing both TSS and hydrocarbon releases into surface water bodies.

REFERENCES

American Society of Testing and Materials (ASTM) (1999). "Standard Test Method for Determining Sediment Concentration in Water Samples," D 3977-97, Vol. 11.02, pp. 389-394.

American Public Health Association (APHA) (1998). "Method 6410 Extractable Base/Neutrals and Acids". *In* Standard Methods for the Examination of Water and Wastewater. 20th Edition. L.S. Clesceri, A.E. Greenberg, A.D. Eaton, Editors. American Public Health Association, American Water Works Association, and the Water Environment Federation. American Public Health Association, Washington, D.C.

ASCE Manuals and Reports of Engineering Practice No. 77 (1992). "Design and Construction of Urban Stormwater Management Systems," American Society of Civil Engineers, New York.

Chen, C.S.H., J.J. Delfino, P.S.C. Rao (1994). "Partitioning of organic and inorganic components from motor oil into water". Chemosphere, 28(7):1385-1400.

Georgia Stormwater Management Manual (2001). Volume 2. Atlanta Regional Commission, Atlanta, GA.

Gwinnett County Stormwater Design Manual (2005). Gwinnett County, Georgia.

Peavy, H.S., Rowe, D.R., and Tchobanoglous, G. (1995). Environmental Engineering, McGraw-Hill, Boston, MA.

U.S. Environmental Protection Agency (EPA) (1996). "Separatory Funnel Liquid-Liquid Extraction Method 3510C", SW-846 On-Line, Test Methods for Evaluating Solid Wastes, Physical/Chemical Methods. Office of Solid Waste, U.S. EPA, Washington D.C. Available at: http://www.epa.gov/epaoswer/hazwaste/test/pdfs/3510c.pdf.

Wanielista, M. P., and Yousef, Y.A. (1992). Stormwater Management. John Wiley & Sons, New York.